Functional Materials 15, No.1 (2008)

Silicon based materials for spintronics prepared by implantation and temperature — (pressure) treatment

Andrzej Misiuk, Lee Chow[*]

Institute of Electron Technology, 46 Al. Lotnikow, 02-668 Warsaw, Poland
[*]Department of Physics, University of Central Florida, Orlando, FL 32816, USA

This work reviews the hitherto published and new results concerning the compositional, structural and magnetic properties of single crystal Si irradiated/implanted with non-magnetic atoms and, especially, with medium dosage ($D \leq 1 \cdot 10^{16}$ cm^{-2}) of V^+, Cr^+ and Mn^+, and subsequently processed at *HT*–(*HP*). The *HT*–(*HP*) treatment affects, among others, the solid phase epitaxial re-growth of amorphous a-Si layer created at implantation. Processed Si:V, Si:Cr and Si:Mn indicate magnetic ordering up to above 300 K. This means that the new Si:V, Si:Cr and Si:Mn materials belonging to the family of Diluted Magnetic Semiconductors have been produced.

Приведен обзор ранее опубликованных и новых результатов, относящихся к составу, структуре и магнитным свойствам монокристаллического Si, облученного/имплантированного немагнитными атомами, в частности, умеренными дозами ($D \leq 1 \cdot 10^{16}$ см$^{-2}$) V^+, Cr^+ и Mn^+, а затем обработанного при *HT*–(*HP*). Обработка *HT*–(*HP*) влияет, помимо других характеристик, на твердофазный эпитаксиальный повторный рост аморфного слоя a-Si, образующегося при имплантации. Обработанные таким образом Si:V, Si:Cr и Si:Mn проявляют магнитную упорядоченность вплоть до температур, превышающих 300 К. Это означает, что возможно получение новых материалов типа Si:V, Si:Cr и Si:Mn, принадлежащих к семейству "разбавленных магнитных полупроводников".

The study of semiconductors containing magnetically active atoms (Diluted Magnetic Semiconductors, DMSs) has been an active research area because of their perspective suitability for spin-transport electronics (spintronics). DMSs combine the electronic properties of semiconductors and memory potential of typical magnetically ordered materials. Most investigations in this field were focused up to now on ferromagnetic III–V compound semiconductors, with manganese as a major dopant. $Ga_{1-x}Mn_xAs$, $In_{1-x}Mn_xAs$ and related materials (GaN:Mn, AlGaN:Mn etc) were among the most comprehensively studied materials [1]. Some other doped semiconductors/insulators (e.g. Mn- or Cu-doped ZnO) have been also reported to be magnetically ordered up to temperatures above room one [2]. More information on these materials as well as on "traditional" Mn-doped III–V semiconductors will be presented in Chapter 1.

Recently, it has been confirmed that single crystal silicon implanted with non-magnetic ions or subjected to neutron irradiation can exhibit specific magnetic properties, with hysteresis loops similar to the those of classic ferromagnetic materials. This specific magnetic ordering has been called tentatively "quasiferromagnetism" [3] (Chapter 2). Magnetically ordered Si-based materials with a high Curie temperature (T_C) would be the best fitting to demands of the modern Si-based microelectronics technology. That is why the paper reporting the above-room temperature ferromagnetism in Mn ion implanted Si (Si:Mn) [4] has been met with interest. Recently, we demonstrated that Si implanted with vanadium or chromium (considered usually as

non-magnetic) also show ferromagnetic ordering [5].

To prepare materials with magnetic ordering, the as-implanted Si:V, Si:Cr and Si:Mn were subjected to post-implantation annealing at elevated temperatures (*HT*), typically under atmospheric pressure (10^5 Pa). This is related to a need to restore the structure of the near surface areas of initially perfect Si single crystal, heavily damaged by implantation. Amorphous silicon (a-Si) is formed under implantation, most abundant near the projected range of implanted ions (R_p). As reported recently [5, 6], enhanced hydrostatic pressure (*HP*) of ambient inert gas effects strongly the re-crystallization (solid phase epitaxial regrowth, SPER) of a-Si and thus the resulting microstructure and magnetic ordering. That is why the effect of *HP* at preparation of magnetically active Si:V, Si:Cr and Si:Mn will be also considered (Chapters 3–5).

1. Mn-doped III–V semiconductors and ZnO doped with transition metals

Dia- or paramagnetic semiconductors or insulators can be transformed into the magnetically ordered ones by including appropriate transitional metal (TM) atoms into their lattice. The current development of spintronic materials was closely related to producing $Ga_{1-x}Mn_xAs$ or $In_{1-x}Mn_xAs$ single crystals (deposited usually by Molecular Beam Epitaxy, MBE, Liquid Phase Epitaxy, LPE, or related techniques) with TC as high as possible. In the case of prototype material, $Ga_{1-x}Mn_xAs$, Ga atoms can be replaced partially by substitutional Mn atoms. The substitutional Mn atoms provide both local magnetic moments and delocalized electron holes. In spite of considerable efforts [7], no satisfying materials with TC much exceeding 150 K have been synthesized. Either ferromagnetism is observed at much below room temperature or no ferromagnetic ordering is detectable. It is worth to mention that HP applied at annealing of InAs/GaAs and similar systems affects strongly their structure [8] and their magnetic properties (these effects are now investigated in details [9]).

The intrinsic morphology of GaAs (InAs) degrades considerably as the TM doping level exceeds 10^{18} cm^{-3}, with precipitates of MnAs being formed [1]. It has been reported [10] that annealing of magnetic III–V semiconductors at *HT*~1000 K results in the formation of multi-phase materials with MnAs as the magnetically active component, with $T_C \geq 290$ K. These materials are now also the subjects of considerable interest [9, 11].

Doped SnO_2, TiO_2, ZnO, and similar insulators also have attracted some attention due to expectation [7] of high magnetic ordering temperatures in the case of their doping with TMs. Such DMSs are of special interest because of interesting optoelectronic properties of ZnO. Room temperature magnetic ordering in polycrystalline Mn doped ZnO has been reported, with magnetization (M) up to $3 \cdot 10^{-3}$ emu/g [12, 13]. Room temperature magnetic ordering has been reported also for micron sized ZnO single crystals doped with 2.2 % Mn (M up to 0.05 emu/g at room temperature) [14]. It has been stated recently that room temperature ferromagnetism in ZnO:Mn can be attributed to substitutional incorporation of Mn at the Zn lattice positions rather than due to the formation of segregated secondary phase [15].

Cobalt doped ZnO polycrystalline ferromagnetic films with T_C up to 750 K were prepared by magnetron co-sputtering [16]; similarly, polycrystalline ZnO films co-doped with Mn and Co have been reported to show ferromagnetic ordering with $T_C \geq 300$ K [17]. Most probably, the presence of Mn as well as of some other TM atoms in ZnO results in exchange interaction between sp-band electrons or holes and the d-electron spins of magnetic dopant atoms. Cu-doped ZnO displays magnetic ordering at room temperatures, too [18]. The origin of this magnetism is still controversial [19]; older results have been reviewed e.g. in [20].

While TM-doped compound semiconductors and oxides exhibit interesting magnetic properties, it is evident that Si-based DMS would have considerable advantage over them as better compatible with the dominating Si-based microelectronics.

2. Quasiferromagnetic Si-based materials

Ferromagnetism related to the presence of dislocations in single crystal Si was reported more than 30 years ago [21]. Ferromagnetic ordering at low temperature in silicon implanted with low energy Ar^+ and Ne^+ has been also reported at the same time [22]. There exists, however, some uncertainty concerning the oldest results reported, mostly because of possible contamination of silicon single crystals available at

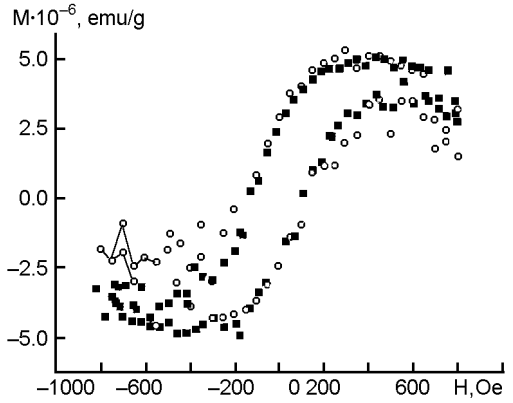

Fig. 1. Ferromagnetic hysteresis loops of Fz-Si:He ($D = 2{\cdot}10^{16}$ cm^{-2}, $E = 150$ keV, $R_p = 1$ μm) processed for 1 h at 723 K under 1.1 GPa, measured at $T = 5$ K (open marks) and $T = 40$ K (black marks).

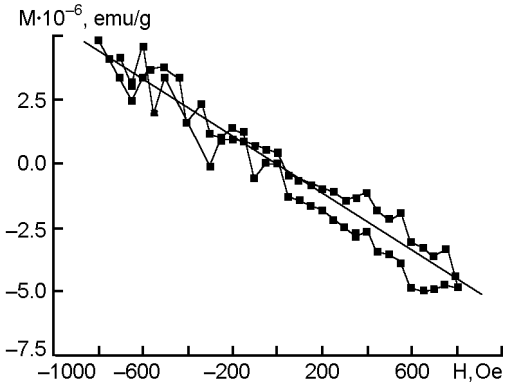

Fig. 2. Magnetization (M) versus magnetic field (H) at $T = 5$ K for Fz-Si:Si ($D = 2{\cdot}10^{16}$ cm^{-2}, $E = 150$ keV) processed for 1 h at 723 K under 1.1 GPa.

that time by ferromagnetic contaminants, including Fe, Co and Ni. Recent results obtained using the modern high purity Si single crystals as the implanted substrate are of much improved reliability in this respect.

The broad magnetic resonance lines (g = 2.2 and 3.4) in Si implanted with high energy Xe^+ ($E = 5.68$ GeV) and Kr^+ ($E = 210$ MeV) were attributed to the formation of the areas with different degree of magnetic order as a result of high energy implantation [23]. It has been considered these signals come from manifestation of internal magnetic fields originating from inclusions with high concentration of unpaired electrons. Recently, ferromagnetic hysteresis loops have been reported at room temperature for single crystal silicon substrates implanted with Si^+ dose, $D = 1{\cdot}10^{16}$ cm^{-2} of or with $D = 2{\cdot}10^{16}$ cm^{-2} of Ar^+, and for Si wafers irradiated with $D = 4{\cdot}10^{16}$ cm^{-2} of thermal neutrons [3]. It has been suggested that the paramagnetic defects (dangling bonds) formed during the implantation or irradiation are responsible for observed magnetic behavior [24]. This type of quasiferromagentism seems to be not limited to the implanted silicon only. Spark-processed silicon [24] and porous silicon [25] also show magnetic hysteresis. As it follows from our recent measurements, a Si sample implanted with He^+ (Si:He, $E = 20$ keV and $D = 1{\cdot}10^{17}$ cm^{-2}), at angle 60° with respect to the substrate normal, indicates signs of magnetic ordering.

In Ferromagnetic Resonance, the frequency dependence of the resonance field, f^2/H versus magnetic field H, follows a straight line as shown by the equation below:

$$\left(\frac{f}{2\pi\gamma}\right)^2 = H_R(H_R + 4\pi M_{eff}).$$

In this equation, the zero-field intercept gives $4\pi M_{eff}$ ($= 4\pi M_s$ when there is no magnetic anisotropy) and the slope, which is related to the gyromagnetic ratio $\gamma = g\mu_B/\hbar$. From γ, the Lande g-factor can be determined.

The in-plane component of the g-factor has been determined to be equal to 2.35. Assuming an isotropic film, a saturation magnetization of $M_s = 1.05$ emu/cm^3 has been estimated.

Ferromagnetic hysteresis loops measured by the SQUID method for Floating zone grown Si implanted with He^+ (Fz-Si:He) and processed at 723 K are presented in Fig. 1.

The as-implanted Fz-Si:Si of a <111> orientation, prepared by self-implantation of Fz-Si with Si^+ ($E = 150$ keV, $D = 2{\cdot}10^{16}$ cm^{-2}) showed a distinct hysteresis of magnetization. However, processing of this sample at 723 K under HP resulted in absence of magnetic ordering (Fig. 2), most probably because of processing-induced recovery of sample crystallinity.

It is quite reasonable to assume that the implantation-induced defects could increase the concentration of unpaired electrons in Si. The processing / annealing of the implanted samples results in gradual recovery of the sample structure and so in decreased concentration of unpaired electrons.

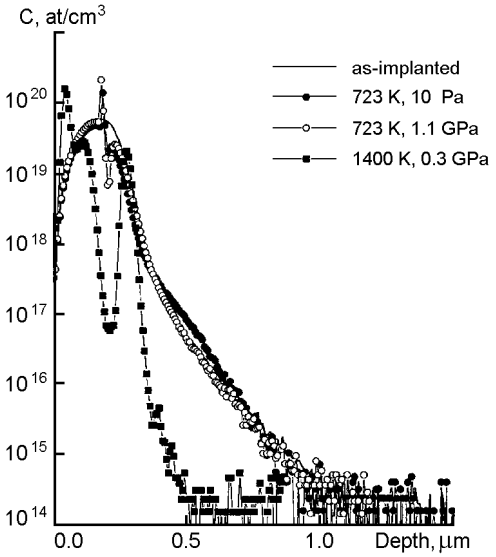

Fig. 3. SIMS depth profiles of V in Cz-Si:V (prepared by V^+ implantation with $D = 1 \cdot 10^{15}$ cm^{-2}, $E = 200$ keV into Czochralski grown silicon, Cz-Si), as-implanted and processed under conditions shown in the Figure.

3. Silicon implanted with vanadium

Similarly as in the case of Si:He and Si:Si, implantation with V^+ produces strongly disordered area near R_p. In the case of $D \geq 10^{15}$ cm^{-2}, amorphization of the Si matrix with the creation of a-Si layer can be expected. For the case $E = 200$ keV and $D = (1-2) \cdot 10^{15}$ cm^{-2}, the total energy introduced during implantation exceeds the amorphization threshold. Therefore, the a-Si layer strongly enriched in vanadium (up to about 0.1 %) has been formed near the surface of single crystal silicon (c-Si) at a depth of about 0.25 μm (Fig. 3). This is evidenced by the presence of a-Si detectable by Transmission Electron Microscopy (TEM) after treatment of Si:V at 610 K. The treatment at up to about 720 K does not result in a detectable recovery of the initial crystallographic perfection of the Si matrix. The Si:V sample processed at 610 K shows a magnetization decreasing a little with increasing measurement temperature, from 5 K to 50 K (Fig. 4, cf. [5]).

At annealing, the a-Si layer is subjected to SPER. This results in the movement of the a-c interface toward the Si surface even at relatively low temperatures (Fig. 3). Since the solubility of V in crystalline Si is very low [27], the V ions are expelled from the re-growth region as the a-Si/crystalline Si interface moves toward the surface.

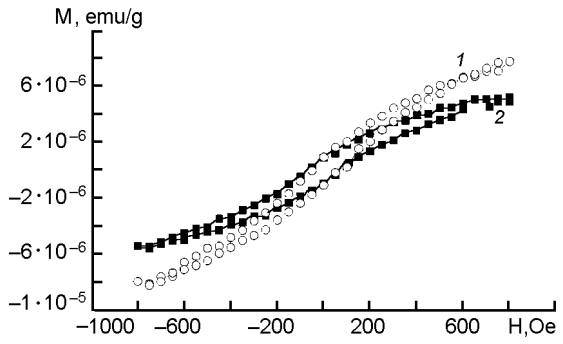

Fig. 4. Magnetization (M) vs magnetic field (H) for Cz-Si:V ($D = 1 \cdot 10^{15}$ cm^{-2}, $E = 200$ keV), processed for 1 h at 610 K under 10^5 Pa. Measurements were performed at $T = 5$ K (*1*) and $T = 50$ K (*2*).

Through this "snow-plow" process, a minimum in the V concentration profile is formed about 0.2 μm below the surface in Si:V processed at 723 K (Fig. 3).

The excess vanadium is accumulated at the a/c interface, and the V concentration reaches a point at which the excess V impurity cannot be pushed away. At higher temperatures (≥900 K), the a-Si layer is converted into polycrystalline state and the silicide VSi_2 is formed [27]. The silicide formation enthalpy amounts 3.2 eV, so VSi_2 remains stable even at high temperatures. A similar V distribution within the near-surface 0.30 μm thick layer evidences that V atoms form silicides (Fig. 3).

As evidenced by X-ray Reciprocal Space Mapping, XRRSM (Fig. 5), SPER of the a-Si layer remains uncompleted after processing at 1270 K.

4. Silicon implanted with chromium

Most results hitherto reported on the properties of silicon implanted with chromium concern Si:Cr prepared by Cr^+ implantation into single crystalline Cz–Si substrate at near-room temperature. In many respects, the behavior of as-implanted and processed Si:Cr reminds that of Si:V. The as-implanted Si:Cr sample ($D = 1 \cdot 10^{15}$ cm^{-2}, $E = 200$ keV) indicates a distinct magnetization with both the saturation magnetization and coercivity depending only slightly on temperature within the 5–50 K range. Similarly as in the case of Cz-Si:V processed at low temperatures, the Cz-Si:Cr samples

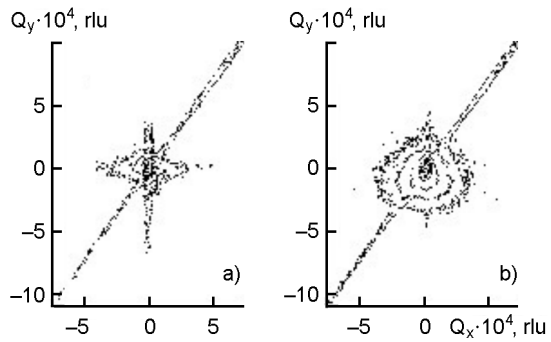

Fig. 5. XRRSM's of Cz-Si:V ($D = 1 \cdot 10^{15}$ cm^{-2}, $E = 200$ keV), processed for 1 h at 1270 K under 10^5 Pa (A) and 1.1 GPa (B).

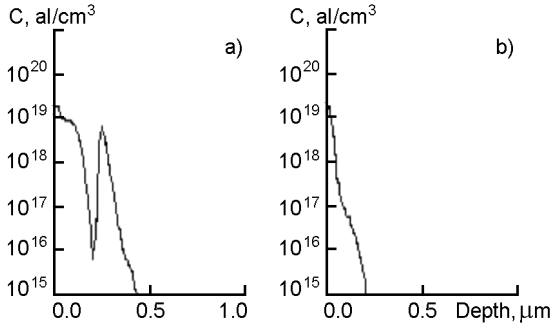

Fig. 6. SIMS depth profiles of Cr in Cz-Si:Cr ($D = 1 \cdot 10^{15}$ cm^{-2}, $E = 200$ keV), processed for 5 h at 1070 K and 1270 K under 10^5 Pa.

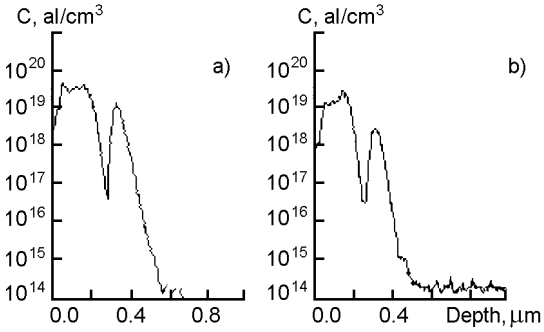

Fig. 7. SIMS depth profiles of Cr in Cz-Si:Cr ($D = 1 \cdot 10^{15}$ cm^{-2}, $E = 200$ keV), processed for 5 h at 1070 K and 1270 K under 1.1 GPa.

processed at ≤723 K indicate ferromagnetic ordering [5, 28].

It is important to mention that magnetization properties of Si:V and of Si:Cr are reflecting the minute size of the ferromagnetic phase present within the sample, composed of thin damaged buried layer enriched in magnetically active implanted atoms. As seen also in the TEM patterns, low-temperature processing of Cz-Si:Cr results in the presence of crystallographic defects within the Si matrix.

SPER of a-Si is much more pronounced at 1070–1270 K (TEM and XRRSM results). No marked structural differences between the re-growth region at the depth <0.30 μm and the single crystal silicon substrate at >0.30 μm depth were detected after processing at 1070 K under 10^5 Pa (Fig. 6). In contrast to Si:V, the diffusion Cr behavior in Si:Cr at 1270 K is strongly affected by *HP* (Figs. 6 and 7, see also [5, 28]).

5. Silicon implanted with manganese

Structural and magnetic properties of silicon implanted with manganese (Si:Mn) were subjected, as so far, to the most extended research [4, 29–32]. Si:Mn samples (D up to $6 \cdot 10^{15}$ cm^{-2}, $E = 300$ keV, $T_s \cong 620$ K) subjected to rapid thermal annealing or short-time annealing (5 min) at up to about 1070 K under 10^5 Pa indicate the presence of ferromagnetic hysteresis loops. The Curie temperature of all samples processed under atmospheric pressure was found to exceed 400 K [4, 29–30]. The saturation magnetization increases with the post-implant annealing temperature attaining 0.2 emu/g at about 1070 K. The out-diffusion of implanted Mn was observed at higher temperatures accompanied by a decrease in the saturation magnetization. It has been suggested that the residual implant damage may play an important role in the observed ferromagnetic ordering of Si:Mn [29, 30].

It has been stated that the substrate temperature and the implanted Mn^+ dose are of great importance for the final structural and magnetic properties of Si:Mn. Processing for 1 h of Si:Mn samples prepared by high dose Mn^+ implantation ($D = 1 \cdot 10^{16}$ cm^{-2}, $E =$ 160 keV, $T_s = 340$ K or 610 K), at ≤720 K both under 10^5 Pa and $HP = 1.1$ GPa results in distinct ferromagnetic ordering [31, 32]. This ordering is detectable up to above room temperature (Fig. 8).

At high-dose Mn^+ implantation ($D \geq 2 \cdot 10^{15}$ cm^{-2}) and for $T_s \leq 310$ K, the Si lattice near R_p in Si:Mn is subjected to complete amorphization. At high temperatures, a-Si is subjected to SPER, depending on annealing temperature, *HP*, and processing time. In the case of Si:Mn prepared by im-

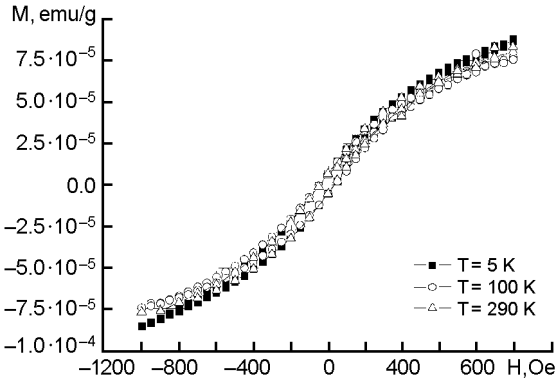

Fig. 8. Magnetization (M) versus magnetic field (H) for Fz-Si:Mn (Fz means Floating zone growth, $D = 1{\cdot}10^{16}$ cm^{-2}, $E = 160$ keV, $T_s = 610$ K), processed for 1 h at 610 K under 10^5 Pa.

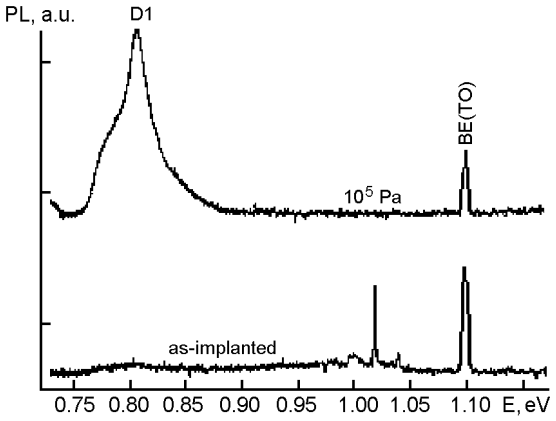

Fig. 9. Photoluminescence (PL) spectra of Fz-Si:Mn ($D = 1{\cdot}10^{16}$ cm^{-2}, $E = 160$ keV, $T_s = 610$ K), as implanted and processed for 1 h at 1070 K under 10^5 Pa.

plantation at $T_s \leq 310$ K, the Si structure recovery (SPER of a-Si) after processing at 1070–1400 K is still incomplete. Depending on the processing conditions, crystallographic defects, such as dislocations (as evidenced by the dislocation-related D1 PL line at about 0.81 eV), were formed (Fig. 9).

It has been stated recently that specific local ordering near the implanted Mn atoms in Si:Mn can be critical with respect to magnetic ordering [33]. No marked effect of the conductivity type on magnetic properties of Si:Mn processed at low temperatures has been stated [34]. In the case of Si:Mn processed at 1070–1270 K, the effect of HP on diffusivity of Mn atoms is especially pronounced. Contrary to the case of Cr in Si:Cr, Mn atoms diffuse faster under HP, especially at 1070 K [31, 32]. In the case of prolonged (1–5 h) annealing under 10^5 Pa and in contrast to earlier observation for the shorter time processed Si:Mn samples [29, 30], some Mn atoms at the >0.25 μm depth remain at the same position as these in the as-implanted sample. Perhaps this is related to the relatively high Mn solubility in Si ($3{\cdot}10^{16}$ cm^{-3} and $3{\cdot}10^{14}$ cm^{-3}, respectively, for Mn and Cr at 1270 K [35]) and to Mn gettering on some implantation-induced defects at the below R_p depth. On the other hand, the presence of tetragonal Mn_4Si_7 (with $T_C \approx 40$ K [36]) in Si:Mn prepared by implantation at $T_s = 610$ K and processed at ≥870 K, has been detected recently [37].

The improved room-temperature ferromagnetism has been also reported for Co- and Mn-ion implanted silicon [38] as well as for Mn-ion implanted Si nanowires [39].

To conclude, our report reviews hitherto published and some unpublished data concerning the composition, structure, and magnetic properties of single crystal silicon implanted with medium dosage of vanadium, chromium and manganese and processed at up to about 1400 K, also under increased hydrostatic pressure, up to about 1.1 GPa. Si:V, Si:Cr and Si:Mn, as implanted and processed at specific conditions, indicate detectable ferromagnetic ordering, with T_C of some Si:Mn samples at above room temperatures. Specific local ordering near the implanted transition metal atoms in Si:M materials (M = V, Cr or Mn) can be critical with respect to the reported magnetic ordering. Still, the observed magnetic ordering in the as-implanted as well as in processed Si:V, Si:Cr and Si:Mn seems to be related in part to the quasi-ferromagnetism observed in silicon implanted with nonmagnetic species and then processed at relatively low temperatures.

To understand the mechanisms of ferromagnetic ordering in ion-implanted Si-based materials, of the formation of specific crystalline magnetically ordered phases and of the origin of quasi-ferromagnetism demands further research. A justified hope could be expressed that new Si–V, Si–Cr and Si–Mn materials belonging to the family of Diluted Magnetic Semiconductors and compatible with Si-based microelectronics will be developed.

Acknowledgements. The authors are thankful to D.Sc.A.Barcz and Mr.M.Prujszczyk from the Institute of Electron Technology, Warsaw, D.Sc.J.Bak-Misiuk and

Dr.W.Osinniy from the Institute of Physics, PAS, Warsaw, M.Sc.B.Surma from the Institute Electron Materials Technology, Warsaw, Poland, and Dr.R.Vanfleet from Brigham Young University, Provo, USA, for experimental assistance, some experimental data and valuable discussion.

References

1. H.Ono, *Physica B*, **376–377**, 19 (2006).
2. O.D.Jayakumar, I.K.Gopalakrishnan, S.K.Kulshrestha, *Physica B*, **381**, 194 (2006).
3. T.Dubroca, J.Hack, R.E.Hummel et al., *Appl. Phys. Lett.*, **88**, 182504 (2006).
4. M.Bolduc, C.Awo-Affouda, A.Stollenwerk et al., *Phys. Rev. B*, **71**, 033302 (2005).
5. A.Misiuk, L.Chow, A.Barcz et al., in: High Purity Silicon 9, Eds: C.L.Claeys, R.Falster, M.Watanabe, P.Stallhofer, ISBN 1-56677-504-3, 2006, p.481.
6. A.Misiuk, B.Surma, J.Bak-Misiuk, *Solid State Phen.*, **108–109**, 351 (2005).
7. T.Dietl, H.Ono, F.Matsura et al., *Science*, **287**, 1019 (2000).
8. J.Bak-Misiuk, A.Shalimov, J.Kaniewski et al., *Cryst. Res. Technol.*, **38**, 302 (2003).
9. J.Bak-Misiuk, A.Misiuk, P.Romanowski, submitted for *Thin Solid Films*.
10. M.Moreno, A.Trampert, B.Jenichen et al., *J. Appl. Phys.*, **92**, 4672 (2002).
11. H.Raebiger, T.Hynninen, A.Ayuela et al., *Physica B*, **376–377**, 643 (2006).
12. P.Sharma, A.Gupta, K.V.Rao et al., *Nat. Mater.*, **2**, 673 (2003).
13. J.Zhang, R.Skomski, D.J.Sellmyer, *J.Appl. Phys.*, **97**, 10D303 (2005).
14. O.D.Jayakumar, I.K.Gopalkrishnan, C.Sudakar, *J. Cryst. Growth*, **294**, 432 (2006).
15. O.D.Jaykumar, I.K.Gopalakrishnan, S.K.Kulshrestha, *Physica B*, **381**, 194 (2006).
16. C.Song, F.Zeng, K.W.Geng, et al., *J. Magn. Magn. Mater.*, **309**, 25 (2007).
17. Y.Wang, Y.Song, S.Yin et al., *Mater. Sci. Engn. B*, **131**, 9 (2006).
18. D.B.Buchholz, R.P.H.Chang, J.H.Song et al., *Appl. Phys. Lett.*, **87**, 082504 (2005).
19. D.J.Keavney, D.B.Buchholz, Q.Ma et al., *Appl. Phys. Lett.*, **91**, 012501 (2007).
20. "Magnetism in Semiconductor Oxides", ISBN 81-7895-264-5, ed. N.H.Hong, Research Signpost (2007).
21. T.Figielski, in: Proc. V Int. Summer School on Defects, Krynica, May 8-18 1976, Polish Sci. Publishers (1978), p.237.
22. A.F.Khokhlov, P.V.Pavlov, *JETP Lett.*, **24**, 211 (1976).
23. S.V.Adashkevich, N.M.Lapchuk, V.F.Stel'makh et al., *JETP Lett.*, **84**, 547 (2007).
24. J.Hack, M.H.Ludwig, W.Geerts et al., *Mater. Res. Soc. Symp. Proc.*, **452**, 147 (1997).
25. R.Laiho, E.Lahderanta, L.Vlasenko et al., *J. Luminescence.*, **57**, 197 (1993).
26. K.S.Jones, S.Prussin, E.R.Weber, *Appl. Phys. A: Solid Surf.*, **45**, 1 (1988).
27. S.P.Murarka, Silicides for VLSI Applications, Academic Press, New York (1983).
28. A.Misiuk, A.Barcz, L.Chow et al., *Solid State Phen.*, **131–133**, 375 (2008).
29. M.Bolduc, C.Awo-Affouda, F.Ramos et al., *J. Vac. Sci. Technol.*, **A24**, 1648 (2006).
30. M.Bolduc, C.Awo-Affouda, A.Stollenwerk et al., *Nucl. Instrum. Meth. Phys. Res. B*, **242**, 367 (2006).
31. A.Misiuk, B.Surma, J.Bak-Misiuk et al., *Mater. Sci. Semicond. Process*, **9**, 270 (2006).
32. A.Misiuk, J.Bak-Misiuk, B.Surma et al., *J. Alloys Comp.*, **423**, 201 (2006).
33. A.Wolska, K.Lawniczak-Jablonska, M.Klepka et al., *Phys. Rev. B*, **75**, 113201 (2007).
34. W.Jung, A.Misiuk, *Vacuum*, **81**, 1408 (2007).
35. H.Francois-Saint-Cyr, E.Anoshkina, F.Stevie et al., *J. Vac. Sci. Technol. B*, **19**, 1769 (2001).
36. U.Gottlieb, A.Sulpice, B.Lambert-Andron et al., *J. Alloys Comp.*, **361**, 13 (2003).
37. J.Bak-Misiuk, E.Dynowska, P.Romanowski et al., *Solid State Phen.*, **131–133**, 327 (2008).
38. P.R.Bandaru, J.Park, J.S.Lee et al., *Appl. Phys. Lett.*, **89**, 112502 (2006).
39. H.W.Wu, C.J.Tsai, L.J.Chen, *Appl. Phys. Lett.*, **90**, 043121 (2007).

Матеріали для спінтроніки на основі кремнію, одержані шляхом імплантації та обробки температурою та тиском

А.Місюк, Лі Чоу

Подано огляд раніше опублікованих та нових результатів, які стосуються складу, структури та магнітних властивостей монокристалічного Si, опроміненого/імплантованого немагнітними атомами, зокрема, помірними дозами ($D \leq 1 \cdot 10^{16}$ см$^{-2}$) V^+, Cr^+ та Mn^+, а потім обробленого при *HT*–(*HP*). Обробка *HT*–(*HP*) впливає, поряд з іншими характеристиками, на твердофазний епітаксіальний повторний ріст аморфного шару a-Si, який утворюється при імплантації. Оброблені таким чином Si:V, Si:Cr та Si:Mn виявляють магнітну впорядкованість до температур понад 300 К. Це означає можливість одержання нових матеріалів типу Si:V, Si:Cr та Si:Mn, які належать до групи "розбавлених магнітних напівпріводників".